J Mater Sci (2012) 47:876–882
DOI 10.1007/s10853-011-5867-z

Microstructure and elastic tensile behavior of polyethylene terephthalate-exfoliated graphene nanocomposites

S. Bandla · Jay C. Hanan

Received: 19 November 2010 / Accepted: 21 February 2011 / Published online: 26 August 2011

Abstract Polyethylene terephthalate-exfoliated graphene nanocomposites were prepared by injection molding. Nanocomposites with graphene platelets of 2, 5, 10, and 15% weight fractions were molded and tested for mechanical characterization. Transmission electron microscopy imaging along with X-ray diffraction show that the graphene platelets remained intact and were dispersed into the matrix. An exponential increase in the Young's modulus of the nanocomposites was observed, but with current limits on exfoliation they do not yet reach the potential suggested by idealized predictions.

Introduction

Polymer nanocomposites (PNCs) have been around for more than two decades [1], they evolved out of the need for lighter and higher performance materials and characterization technologies appropriate for their small scale interactions. Nanoreinforcements have advantages over larger reinforcements. As explained by Fukushima [2], based on the Griffith crack theory and Weibull analysis, smaller particles are stronger and can be more effective in reinforcing the matrix compared to their larger counter parts [3]. Also, with their increased surface area and high aspect ratios, lower volumes of smaller reinforcements can provide equivalent reinforcement. Nanoparticle selection will be based on the required properties, interaction with the matrix, processing, cost, and application of the final composite. Several nanoparticles such as organoclays (MMT), metal nanoparticles (Al, and Ag), metal oxides (ZnO, silica), and carbon derivatives (CNT's, fullerenes, graphite oxide, graphene) have been investigated for the preparation of PNCs [4, 5].

Graphene (a monolayer of carbon atoms) has excellent mechanical (modulus—1060 GPa, strength—20 GPa) and electrical properties (50×10^{-6} Ω cm), compared with other nano particles [2]. However, relatively few investigations in the field of nanocomposites exist, partially due to difficulties associated with large scale production [6, 7]. Graphene has been shown to disperse well in polymers through the aid of surface treatments. Recently, several researchers have been working on the development of PNCs using different forms of graphite (graphite [8], graphite oxide, exfoliated graphite (EG) [9, 10], graphene platelets [11]). Jang et al. [7] detailed the process of exfoliation of graphite, through different fundamental approaches. Exfoliated graphene nanoplatelets (xGnP), multiple graphene layers stacked to form platelets, were developed by a cost effective method, as mentioned by Fukushima [2]. Researchers such as Kalaitzidou et al. [12], Miloaga et al. [13] have investigated the application of graphene nanoplatelets as a reinforcement with different polymers.

Even with years of knowledge in the field of PNCs, a lack of complete understanding on the interactions between the polymer matrix and nanoreinforcements and an efficient method suitable for large scale production remains. Not many PNC's exist in the commercial domain. Manufacturing processes such as melt compounding, solid-state shear pulverization (SSSP) [8], in situ microemulsion polymerization [14], master batch processing [15], have

Electronic supplementary material The online version of this article (doi:10.1007/s10853-011-5867-z) contains supplementary material, which is available to authorized users.

S. Bandla · J. C. Hanan (✉)
Mechanical & Aerospace Engineering,
Oklahoma State University, Tulsa, OK 74106, USA
e-mail: Jay.Hanan@okstate.edu

been attempted with different polymers, however, only few are suitable for large scale production. Selection of the process depends on the matrix resin and type of the nanoparticles used.

Continuous fiber composites are often assessed based on a simplified empirical formula, referred to as the 'Rule of Mixtures'. In the case of nanoreinforcements, the 'Rule of Mixtures' either under-estimates or over-estimates the final properties. This can be because of their low volume fractions and often greater disparity of properties between the matrix an reinforcement. For nanocomposites, the special interaction between the nanoplatelets and matrix is important in determining their elastic behavior. High aspect ratios of the nanoplatelets combined with complex mechanisms at the matrix-reinforcement interface complicate nanocomposite property estimation. Therefore, traditional micromechanical models have been modified to estimate the mechanical properties for nanoparticles [16].

As a part of this work, PET-exfoliated graphene nanocomposites were prepared using injection molding through a master batch process, where graphene nanoplatelets were compounded with PET to form master batch pellets. Compounding involves shear mixing of the resin and nanoplatelets using a double screw extruder. Specific screw designs help in the dispersion of platelets, by altering the applied shear intensities. Master batches provide advantages on material handling and further ease mixing of PET-graphene pellets.

Polyethylene terephthalate is primarily used for fibers, with the majority of production in Asia [17]. PET also finds application as injection molded parts which also benefit from biaxial stretching through secondary operations. Making PET matrix composites with improved properties over neat PET will help in expanding the range of product usage. Also, with increased environmental stewardship, reinforcing offers a path for reduced volume of polymer usage per product; and stiffer products reduce waste during high speed manufacturing. PET also benefits from its clear appearance. Potentially, effective dispersion of nanoparticles in at least small volume fractions should not significantly alter the visible properties (such as transparency).

Polyethylene terephthalate nanocomposites have been reported using different nanoparticles (clay [18], CNT [19]), Zhang et al. [20] have investigated electrical conductivity of PET-graphene nanocomposites. This is the first paper that reports the mechanical properties of PET-exfoliated graphene nanocomposites. These experimental results were compared to theoretical performances using Halpin-Tsai and Hui-Shia models.

Experimental

Materials

In this work, commercially available polyethylene terephthalate of 0.80 dl/g (I.V.) called oZpet™ (GG-3180 FGH, by Leading Synthetics, Australia) was used. Exfoliated Graphene Nanoplatelets, xGnP®-M-5 grade (99.5% carbon) of average diameter 5 μm as shown in Fig. 1, were obtained as dry powder from XG Sciences, Inc. (East Lansing, MI). Graphene nanoplatelets (xGnP) and the as received PET resin were compounded into PET-xGnP master batch pellets by Oviation Polymers (Medina, OH) using their ExTima™ technology. Graphene nanoplatelets are hydrophobic in nature; effective dispersion of graphene results from the interaction of oxygen and hydroxyl functional groups (formed due to the exposure of raw carbon during the fracture of platelets) on their surface with polar groups of PET [20]. Master batch pellets (1.5 mm in diameter and 2 mm height) obtained from the above process were used as raw material for the injection molding process. PET control samples and PET-xGnP nanocomposite tensile bars of increasing weight fractions (2, 5, 10, and 15%) were injection molded at 250–260°C temperature, following type-I specifications of ASTM D 638.

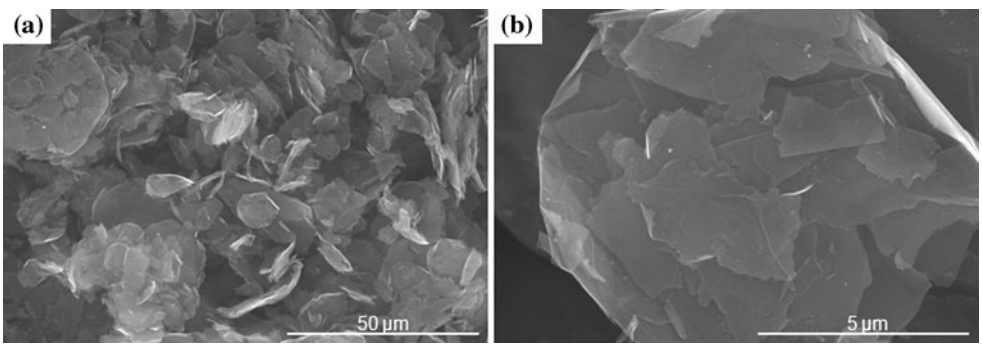

Fig. 1 SEM micrographs of xGnP powder sample **a** ×1000, **b** ×11000

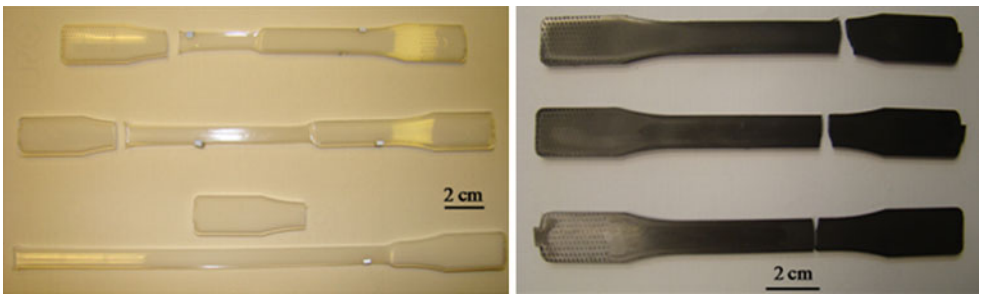

Fig. 2 Tensile tested samples of PET (*left*) and PET-15% xGnP nanocomposite (*right*)

Characterization techniques

The nanocomposite tensile bars (shown in Fig. 2) were tested using a universal materials tester (Instron 5582 model). Tests followed the ASTM D 638 standard at a cross-head speed of 5 mm/min. A non-contact Laser Extensometer (Electronic Instrument Research, Model LE-05) was used to record displacement free of machine compliance. The laser extensometer records displacement of reflections from the self reflective stickers placed at the gauge length. Three composites of each kind were tested along with neat PET specimens for comparison. The laser displacement and load from the crosshead were simultaneously recorded at a time interval of 100 ms.

Dispersion of the graphene nanoplatelets was observed using electron microscopy (SEM, TEM) and X-ray diffraction. SEM micrographs of the xGnP powder and the fracture surfaces of the PET, and PET-exfoliated graphene nanocomposites were obtained using a Hitachi S-4800. The PET control and the nanocomposite with lower graphene content were Au/Pt coated using a Balzers Union MED 010 coater. Thin sections (thickness of 70 nm) used for transmission imaging were microtomed using Reichert-Jung Ultracut E microtome. Transmission micrographs were collected using a JEOL JEM-2100 microscope, with an operating voltage of 200 kV. X-ray diffraction patterns were collected in reflection, on a Bruker D8 Discovery diffractometer, using Cu K_α ($\lambda = 1.54054$ Å) radiation. XRD scans of the xGnP powder along with the PET samples were collected at 40 kV and 40 mA with an exposure time of 120 s.

Results and discussion

Scanning electron microscopy

SEM micrographs of the xGnP dry powder shown in Fig. 1b shows an agglomerated platelet, with each platelet comprised of numerous graphene layers stacked together. These platelets were of 5 to 10 μm average diameter and several nanometers (5–20 nm) in thickness. Micrographs (Fig. 3b–f) of the PET-graphene nanocomposite failure surfaces showed that the graphene nanoplatelets remained

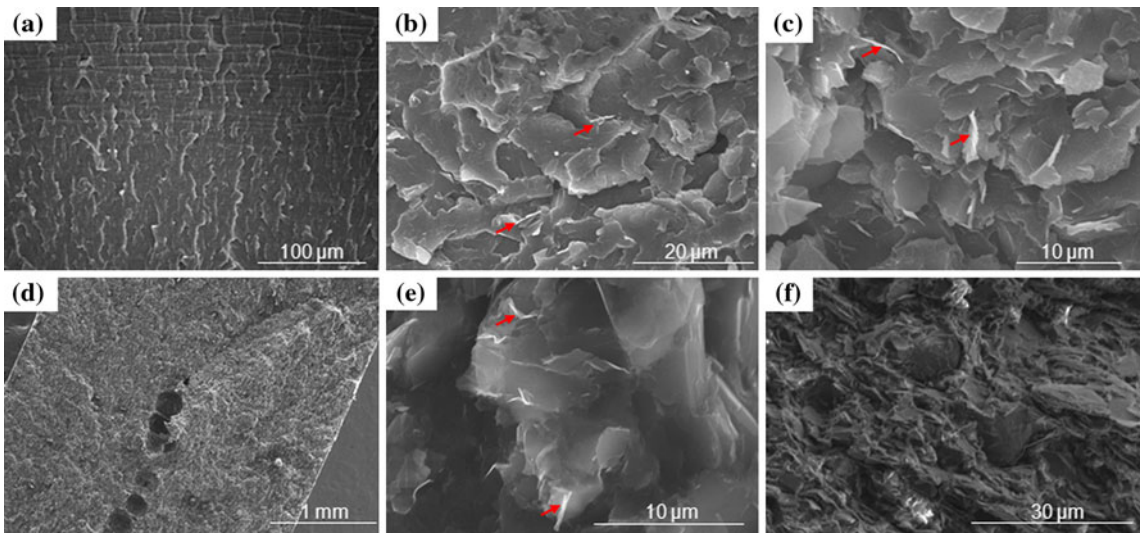

Fig. 3 SEM micrographs of **a** PET, PET-xGnP nanocomposite, **b** 2 wt%, **c** 5 wt%, **d** 10 wt% with micro voids, **e** 10 wt% at 5 k× and **f** 15 wt% samples

intact and were dispersed into the PET matrix, with no signs of agglomeration. The micrographs elucidate that the failure of the nanocomposite under tensile loading was through coalescence of brittle micro-fractures. The presence of micro voids and the initiation of cracks from these voids can be noticed from the SEM micrographs of nanocomposite samples with 5 and 10% graphene nanoplatelet weight fraction. SEM micrographs show the nanoplatelets were projecting out of the fracture surfaces. They appear to be deformed and mixed with the matrix.

Transmission electron microscopy

The performance of nanocomposites depends on dispersion of the nanoparticles. TEM micrographs were collected from 70 nm thin sections to gain better understanding of nanoplatelet dispersion. The transmission micrographs shown in Fig. 4, revealed the graphene nanoplatelets remained intact as platelets and were dispersed into the polymer matrix, individual dispersion of graphene sheets (complete exfoliation) was not found. Micrographs were collected in both bright and dark field modes. As the nanoplatelets consist of several individual graphene sheets, the 70 nm thick sections used may contain layers of polymer and graphene platelets, therefore dark field mode was advantageous. Graphene is more conductive than the polymer matrix so, in transmission imaging, this difference provides contrast.

X-ray diffraction

XRD patterns collected from the dry xGnP powder, PET control, and PET-xGnP nanocomposite are shown in Fig. 5. The diffraction pattern for the graphene nanoplatelets shows the Graphene-2H characteristic peaks at 26.6° ($d = 3.35$ Å) and 54.7° ($d = 1.68$ Å) 2θ. Slight broadening of the peak at 26.6° 2θ indicates the presence of platelets with different dimensions. A broad amorphous peak from the PET control sample was observed around 19.2° 2θ. This confirms the control sample has an amorphous microstructure. As shown in Fig. 5, the intensity of the Graphene peak at 26.6° 2θ increased with the weight fraction of the nanoplatelets. No peak shift was observed. This along with the TEM micrographs confirms that the nanoplatelets were not substantially exfoliated [21]. Further, the diffraction pattern confirms the PET matrix was amorphous as expected, at least within 0.2 mm of the surface.

Mechanical behavior

Stress–Strain curves for the PET control and nanocomposite were plotted as shown in Fig. 6, based on the data collected from the tensile tests. The addition of graphene nanoplatelets has increased the performance (modulus) over the pure PET up to 300% and follows an exponential trend as shown in Fig. 7. While primarily linear behavior is observed, a hump in the stress strain curve for the 15% nanocomposite, suggests an additional toughening mechanism for this composite over the other lower volume

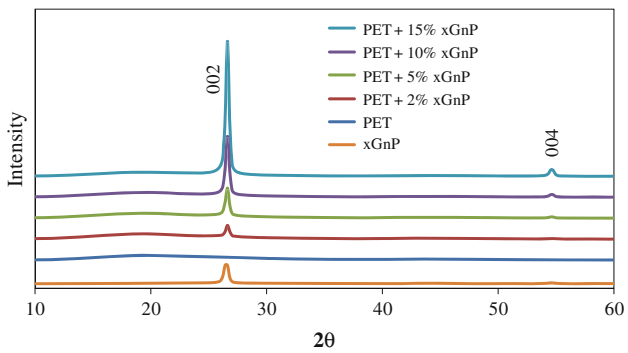

Fig. 5 Comparison of XRD patterns of xGnP powder with PET control and nanocomposite

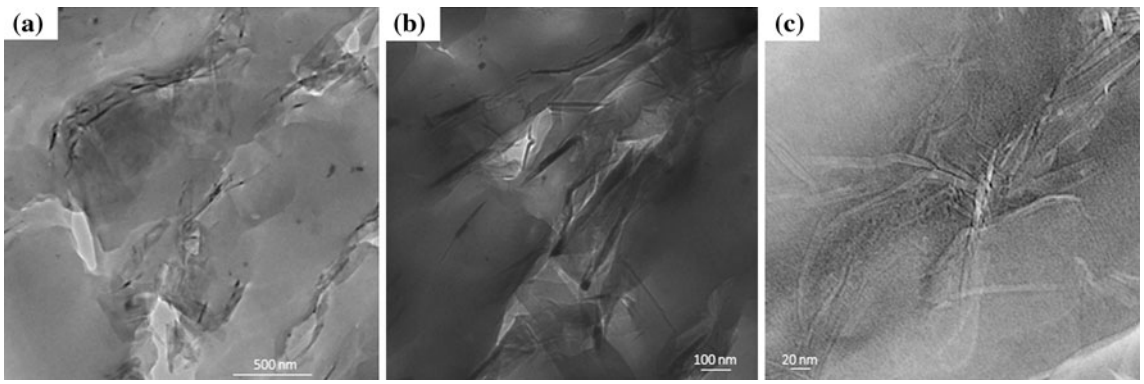

Fig. 4 TEM micrographs showing dispersion of the nanoplatelets in PET-15% xGnP nanocomposite; bright field images **a** 10 k×, **b** 20 k×, and **c** dark field image at 60 k×

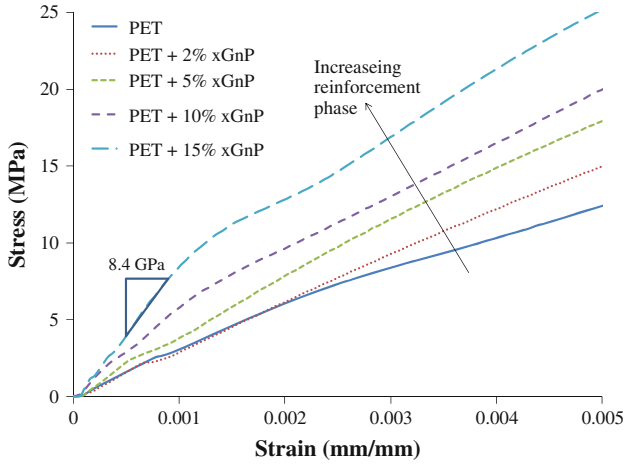

Fig. 6 Comparison of stress–strain curves of PET and PET-xGnP nanocomposites

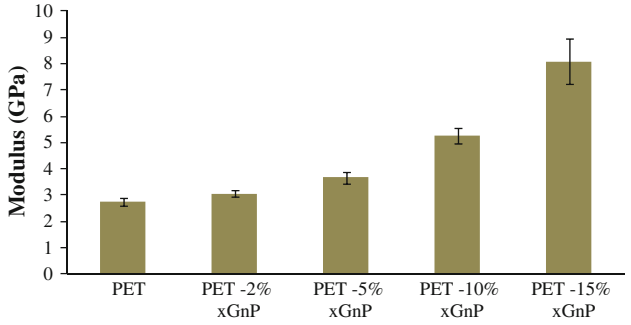

Fig. 7 Young's modulus of PET nanocomposites in comparison with control PET

fraction. This may be due to a reinforcement–reinforcement interaction.

With the objective of understanding the effectiveness of graphene nanoplatelets as reinforcement, micromechanical models such as the Halpin-Tsai and the Hui-Shia models were used to determine the theoretical elastic mechanical performance of this PET-graphene nanocomposite. Micromechanical models estimate the properties based on assumptions, such as perfect reinforcements, homogenous dispersion, or consistent orientation of the reinforcements. An ideal case for superior performance of the graphene nanocomposite is to have defect free graphene sheets (monolayers) of the required length well dispersed into the matrix and orientated along the direction of maximum load.

Gong et al. [16] have determined a required length for graphene platelets (>30 μm) to be effective as reinforcement. Mechanical properties of the graphene platelets such as stiffness and poisson's ratio decrease with increase in the number of comprising layers, as observed by Georgantzinos et al. [22] with molecular simulations. They estimated that the stiffness of platelet comprising five layers decreases by 15% compared to single layer graphene, and they also noticed that the properties of the graphene differ based on their orientation. Modulus of the graphene platelet (flake) has been reported as 0.795 TPa [23].

In this work, graphene platelets with a wide range of length (or diameter of the platelets present in the out of plane direction) and thickness were observed from the TEM micrographs. The change of particle size from the larger (5 μm) dry graphene powder to the smaller (300 nm), size as observed in the TEM images (Fig. 4) can be due to shearing during the compounding and molding process. Table 1 shows the average size of the platelets with minimum and maximum values. These platelet properties were then used in determining the performance range of the nanocomposites, based on the micromechanical models (error bars shown in Fig. 8). Predicted moduli of the nanocomposite from the micromechanical models were plotted against the experimental results, shown in Fig. 8. The modulus estimated through the Halpin-Tsai model is higher compared to the experimental value. The Halpin-Tsai model estimates the modulus of the composite with platelets being aligned along the loading direction. However, the platelets were not generally aligned in the direction of the loading. In addition, extremely high stiffness of the reinforcement compared with the matrix (>250×), make difficult accurate predictions through the Halpin-Tsai model [22]. The Hui-Shia model shows the best agreement. The Hui-Shia model estimates elastic modulus of the nanocomposite with platelets loaded both in parallel (axes 1 and 2) and perpendicular directions (along axis 3) as shown in Fig. 8. This model is valid for wide range of stiffness ratios over the Halpin-Tsai model [22].

In addition, stress transfer between the matrix to reinforcement in composites is critical in controlling their mechanical behavior. For example, graphene nanocomposites in PMMA matrix, the stress transfer between the

Table 1 Properties of graphene and PET used for theoretical predictions

Graphene platelet properties				PET properties
Average length/diameter (*D*) nanometers (min/max)	Average thickness (*t*) nanometers (min/max)	Aspect ratio (*D*/*t*)	Modulus (GPa)	Modulus (GPa)
300 (28/730)	16 (3/28)	18.75	795	2.7

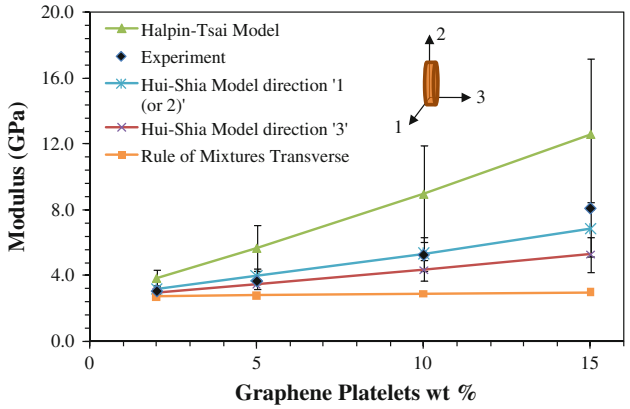

Fig. 8 Modulus of PET-graphene nanocomposites from predictions compared with experimental results

matrix and graphene platelets and graphene–graphene sheets were shown dominated by week van der Waals forces [16], reducing the potential mechanical performance. However, micromechanical models do not account these changes in stress transfer behavior. This results a deviation from the experimental values.

The current experimental modulus showed reasonable agreement with theoretical predictions. This is in spite of the broad range in platelet geometry (see table). The best case was the Hui-Shia model with the modulus parallel to the platelet (direction-3). This suggests reasonable effectiveness of the reinforcement. With the reinforcement distributed randomly, behavior between the two Hui-Shia predictions of parallel and perpendicular might be expected. Further investigation to the randomness of the platelet distribution is needed for additional assessment. Even stiffer modulus enhancement could be expected if the platelets were of higher aspect ratio as the modulus predicted are sensitive to the aspect ratio. This is a reasonable goal with continued improvement in the production of the additives and their processing with the matrix. Clearly, nanoscale reinforcement is a benefit to the enhancement of mechanical properties.

Furthermore, from X-ray diffraction, the addition of graphene platelets does not show an impact on the final crystallization of PET. Economies of scale can improve the cost of any of these additives. More understanding of the effect nanoplatelets have on the injection molding process can help improve the composite properties further. For example, many different screw types are available for injection molding and need to be explored for their advantages in mixing and dispersion of additives.

Conclusions

Graphene nanoplatelets were effective in achieving an improved elastic modulus for poly (ethylene terephthalate). Injection molding of master batch pellets was successfully employed for the preparation of PET-exfoliated graphene (xGnP) nanocomposites of weight fractions from 2 to 15%. Comparison with simple mechanical models suggests their superior performance. The stiffness is not only dependent on the reinforcement stiffness, but also on its aspect ratio and the dominating mechanism for interfacial stress transfer between matrix and reinforcement. There is also some indication that the reinforcement–reinforcement interaction plays an important role as the volume fraction exceeds 10%. Further progress on the process used for exfoliation of graphene nanoplatelets can help in scaling up for industrial applications.

Future work

Further investigation for understanding the interaction between PET and graphene nanoplatelets is needed. An ability to further disperse the exfoliated platelets is an important next step shared with many nano-reinforcements.

Acknowledgements We acknowledge XG Sciences for providing xGnP-M-5 grade nanoplatelets and Oviation Polymers for compounding and injection molding of the samples. We also, acknowledge Mr. Terry Colberg, OSU Microscopy Lab, for his help with microtome and TEM imaging and Au/Pt coating of samples for SEM. This work is part of an industry sponsored research program at Oklahoma State University.

References

1. Kuila T, Bhadra S, Yao D, Kim NH, Bose, Lee JH (2010) Prog Polym Sci 35(11):1350
2. Fukushima H (2003) Graphite nanoreinforcements in polymer nanocomposites. PhD Dissertation, Department of Chemical Engineering and Materials Science, Michigan State University, p. 311
3. Jiang X, Drzal LT (2009) Polym Compos 31:1091
4. Hussain F, Hojjati M, Okamoto M, Gorga RE (2006) J Compos Mater 40:1511
5. Paul DR, Robeson LM (2008) Polymer 49:3187
6. Schniepp HC, Li J-L, McAllister MJ, Sai H, Herrera-Alonso M, Adamson DH, Prud'homme RK, Car R, Saville DA, Aksay IA (2006) J Phys Chem B 110:8535
7. Jang B, Zhamu A (2008) J Mater Sci 43:5092. doi:10.1007/s10853-008-2755-2
8. Wakabayashi K, Pierre C, Dikin DA, Ruoff RS, Ramanathan T, Brinson LC, Torkelson JM (2008) Macromolecules 41:1905
9. Kim IH, Jeong YG (2010) J Polym Sci B 48:850
10. Uhl FM, Yao Q, Nakajima H, Manias E, Wilkie CA (2005) Polym Degrad Stab 89:70
11. Rafiee MA, Rafiee J, Wang Z, Song H, Yu Z-Z, Koratkar N (2009) ACS Nano 3:3884
12. Kalaitzidou K, Fukushima H, Drzal LT (2007) Compos Sci Technol 67:2045
13. Miloaga DG, Hosein HAA, Misra M, Drzal LT (2007) J Appl Polym Sci 106:2548

14. Patole AS, Patole SP, Kang H, Yoo J-B, Kim T-H, Ahn J-H (2010) J Colloid Interf Sci 350:530
15. Li YC, Chen GH (2007) Polym Eng Sci 47:882
16. Hu H, Onyebueke L, Abatan A (2010) J Min Mater Charact Eng 9:45
17. Beale PA (2011) In: The packaging conference, Las Vegas
18. Chang J-H, Kim SJ, Joo YL, Im S (2004) Polymer 45:919
19. Anand K, Agarwal A, Joseph R (2007) Carbon nanotubes-reinforced PET nanocomposite by melt-compounding. J Appl Polym Sci 104:3090
20. Zhang H-B, Zheng W-G, Yan Q, Yang Y, Wang J-W, Lu Z-H, Ji G-Y, Yu Z-Z (2010) Polymer 51:1191
21. Morgan AB, Gilman JW (2003) J Appl Polym Sci 87:1329
22. Hui CY, Shia D (1998) Polym Eng Sci 38:774
23. Blakslee OL, Proctor DG, Seldin EJ, Spence GB, Weng T (1970) J Appl Phys 41:3373